



CHORUS

This is the accepted manuscript made available via CHORUS. The article has been published as:

Gradient Catastrophe and Fermi-Edge Resonances in Fermi Gas

E. Bettelheim, Y. Kaplan, and P. Wiegmann

Phys. Rev. Lett. **106**, 166804 — Published 20 April 2011

DOI: [10.1103/PhysRevLett.106.166804](https://doi.org/10.1103/PhysRevLett.106.166804)

Gradient Catastrophe and Fermi Edge Resonances in Fermi Gases

E. Bettelheim,¹ Y. Kaplan,¹ and P. Wiegmann²

¹*Racah Institute of Physics, Hebrew University, Jerusalem, Israel*

²*The James Franck Institute, University of Chicago*

Any smooth spatial disturbance of a degenerate Fermi gas inevitably becomes sharp. This phenomenon, called *the gradient catastrophe*, causes the breakdown of a Fermi sea to multi-connected components characterized by multiple Fermi points. We argue that the gradient catastrophe can be probed through a Fermi edge singularity measurement. In the regime of the gradient catastrophe the Fermi edge singularity problem becomes a non-equilibrium and non-stationary phenomenon. We show that the gradient catastrophe transforms the single-peaked Fermi edge singularity of the tunneling (or absorption) spectrum to a sequence of multiple asymmetric singular resonances. An extension of the bosonic representation of the electronic operator to non-equilibrium states captures the singular behavior of the resonances.

1. Introduction The FES (Fermi edge singularity [1–3]), observed as a power law peak in the absorption spectrum of X-rays in metals more than 70 years ago, is one of the most prominent and well understood quantum many-body phenomena caused solely by Fermi statistics.

FES also has been demonstrated in tunneling experiments [4–7]: a sudden switch-on of a contact potential due to a change in the capacity of the contact in tunneling causes a power law dependence of the tunneling current on the bias voltage: $I(V) \sim V^{-2a+ka^2}$ [8]. Here $\delta = \pi a$ is the scattering phase of the ensuing potential and k is the number of scattering channels. In the case of an attractive potential ($a > 0$) the current peaks at the Fermi edge.

The physics of the FES is explained by the phenomenon of the Orthogonality Catastrophe [9]: the state of a Fermi gas $\langle \Omega' |$ after a localized potential is suddenly switched on, is almost orthogonal to a state of the unperturbed Fermi gas $|\Omega\rangle$. Their overlap vanishes with the level spacing Δ as a power law $\langle \Omega' | \Omega \rangle \sim (\Delta/E_F)^{ka^2}$.

The FES acquires new features in the non-stationary regime due to the *gradient catastrophe*. A gradient catastrophe is a hydrodynamic instability observed in many classical (and, recently, in atomic) systems. In Ref. [10] it has been shown that a quantum analog of the gradient catastrophe also takes place in a degenerate Fermi gas. The ballistic propagation of macroscopical packets and fronts in Fermi gases inevitably enters the gradient catastrophe regime, where the initially smooth fronts develop large gradients and undergo a shock wave phenomenon: packets overturn as shown in Fig 1. The observation of non-stationary phenomena in Fermi gases may not be easy since electronic times are too short, but does not seem impossible. From the theoretical viewpoint a non-stationary FES reveals important (and new) aspects of the Orthogonality Catastrophe. Both catastrophes are caused solely by Fermi statistics and therefore their interaction is of interest.

The physics of non-stationary processes in Fermi gases is in its infancy. Ref. [10] discusses oscillatory corrections to the Orthogonality Catastrophe in a non-stationary regime: the overlap of the state of a shaken-up Fermi

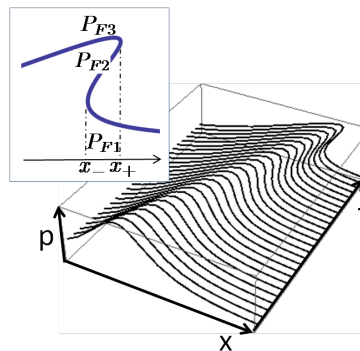


FIG. 1: Time progression of the Fermi edge. The front overhangs, giving rise to three Fermi (see inset) edges ($P_{F3} > P_{F2} > P_{F1}$) between the trailing (x_-) and leading (x_+) edges.

gas with a propagating packet (both before and after the shock). We also mention Refs. [11] which cast non-stationary Fermi gases in the context of integrable nonlinear waves.

In this paper we study the FES in a non-stationary regime before and after the quantum shocks had occurred. We show that each shock introduces two additional Fermi edges, each edge causes an additional resonance peak schematically depicted in Fig. 2. In general settings we predict that a smooth wave packet passing through a tunneling contact shows a sequence of singular pulses in the tunneling current. Here we discuss only one shock, though the extension to multiple shocks is straightforward.

Non-stationary FES in its generality consists of several different regimes some of them are difficult to study. In this paper we consider a regime away from turning points. There the Fermi surface changes much slower than the Fermi scale. In this case the problem becomes quasi-stationary and can be solved in two steps. First we neglect the time dependence of the Fermi points leading to FES problem with a non-equilibrium population of electronic states. Once this has been done, we may treat the Fermi-edges as slow time dependent variables. We argue that they obey the Riemann equation.

The stationary non-equilibrium FES problem has been

extensively studied in Refs. [12] and more recently in Refs. [13–15], so we could have borrowed the results. We suggest instead a simple compact approach to problem, using a generalization of the bosonization approach. In a related paper [15] we formulate the non-equilibrium FES problem as a matrix Riemann-Hilbert problem with an integrable kernel.

2. *Tunneling in a non-stationary regime.* We consider the following situation:

(i) A Fermi gas is in contact with a localized resonant level (a quantum dot). It is initially uncharged and provides no scattering to electrons. When an electron tunnels to the dot, it suddenly charges the dot, switching-on a small potential $H \rightarrow H' = H + U$ localized at the dot [8]. We assume the potential is weak, such that the scattering phase $|\delta| < \pi/2$ and therefore $|a| < 1/2$. Assume no further interaction, no dissipation, ignore spin and channels.

(ii) A semiclassical electronic front or a packet - a state with a spatially inhomogeneous density matrix ϱ has been initially created in a Fermi gas as it is shown in Fig. 1 [10].

This setting can be realized in different ways. For example, a smooth potential well, trapping a large number of electrons, is suddenly removed. The electronic packet thus released propagates towards the dot, eventually hits it, facilitating tunneling. Alternatively, one may apply a time dependent voltage through a point like contact separated from the dot [16].

The state which is thus created is a coherent state. It can be understood as a state having a spatially varying Fermi point, $P_0(x)$. $P_0(x)$ is assumed to change slowly on the Fermi scale, $\hbar|\nabla P_0|/P_0 \ll P_F$. This condition justifies the semiclassical analysis described below.

The tunneling current is given by the golden rule [1, 8]. In units of a tunneling amplitude $I(\omega)|_{\hbar\omega=eV+E_F}$ reads

$$I(\omega, t) \propto \text{Re} \int_0^\infty e^{i\omega\tau} G(t + \frac{\tau}{2}, t - \frac{\tau}{2}) d\tau, \quad (1)$$

$$G(t_1, t_2) = \langle \Omega | e^{iHt_2} c e^{iH'(t_1-t_2)} c^\dagger e^{-iHt_1} | \Omega \rangle \quad (2)$$

Here $c = \sum_k e^{-ikx_0} c_k$ and x_0 is the position of the dot.

Since all the physics is concentrated at the Fermi edge

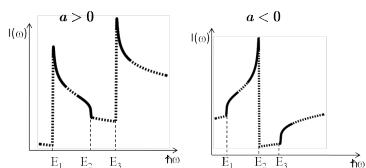


FIG. 2: A schematic plot of the tunneling current for $a > 0$ (left panel) and $a < 0$ (right panel), solid lines show computed power law asymptotes. Dashed lines interpolate between resonances. $a < 0$ displays a single peak after the shock, while $a > 0$ displays two peaks.

a knowledge of the dispersion at the edge is sufficient

$$\epsilon_p = E_F + v_F(p - P_F) + \frac{(p - P_F)^2}{2m} + \dots \quad (3)$$

In the literature the parabolic part of the dispersion is routinely ignored. In this approximation our effect disappears [17].

We evaluate $G(t_1, t_2)$ in the regime where the typical time of tunneling $\tau = t_2 - t_1 > 0$ is much smaller than the time it takes for the packet to change. This approximation does not allow us to compute the broadening of the resonance at the frequency range $\gamma \sim v_F(\nabla P_0/\hbar)^{1/2}$, but it captures the power law shoulders of resonances and their dependence on time t .

Under this assumption during the short time of tunneling the energy dependence of the Fermi velocity and scattering phase δ caused by the potential U can be dropped in some interval $|\epsilon - E_F| \ll \Lambda$ at the Fermi edge, where the cut-off Λ (typically of the Fermi scale) is assumed to be larger than $v_F P_0$ and \hbar/τ . This amounts a shift of energy levels after scattering downwards by a constant amount a (in units of level spacing): $\epsilon_p \rightarrow \epsilon_p - a$.

In Ref. [18] it has been shown that the vertex operator $e^{a\varphi}$ implements a shift of momenta such that a perturbed Hamiltonian and perturbed states are $H' = e^{-a\varphi(x_0)} H e^{a\varphi(x_0)}$ and $|\Omega'\rangle = e^{a\varphi(x_0)} |\Omega\rangle$. Then Green's function reads

$$G(t_1, t_2) = \langle \Omega | c(t_2) e^{-a\varphi(x_0, t_2)} e^{a\varphi(x_0, t_1)} c^\dagger(t_1) | \Omega \rangle. \quad (4)$$

This formula is standard. The only difference is that the density matrix does not commute with the Hamiltonian and therefore the process is not-stationary - the Green function and a current depend on $t = 1/2(t_1 + t_2)$.

3. *Gradient Catastrophe: Riemann equation for Fermi Gases.* We demonstrate the gradient catastrophe on the evolution of the Wigner function - a simpler object than (2). The Wigner function describes occupation in phase space:

$$n_F(x, p, t) = \int \langle \Omega | c^\dagger(x + \frac{y}{2}, t) c(x - \frac{y}{2}, t) | \Omega \rangle e^{-\frac{i}{\hbar} p y} dy \quad (5)$$

We assume that the front is plane or radial, such that the dynamics is essentially one dimensional and chiral.

Semiclassically, the Wigner function is equal to 1 in a bounded domain $p < P_F(x, t)$ of the phase space (p, x) - the Fermi sea - and vanishes outside the Fermi sea $n_F(x, p, t) \approx \Theta(P_F(x, t) - p)$. This form is valid as long as the gradients of the spatial dependence of the Fermi momentum $P_F(x, t)$ are small [20]. The shape of the initial Fermi surface is given by the density matrix $P_F(x, 0) = P_F + P_0(x)$. The support of the Wigner function is the area below the Fermi surface in Fig. 1.

How does the Fermi surface change in time? It does not, if one neglects dispersion of the Fermi gas, i.e., treats the velocity $v_p = d\epsilon_p/dp$ as a constant: the front translates with the Fermi velocity without changing its shape.

It does change, in a dramatic fashion, if the dispersion in (3) (no matter how small) is taken into account.

The Wigner function (for a dispersion $\epsilon_p = p^2/2m$) obeys the equation

$$(\partial_t + v_p \nabla) n_F(x, p, t) = 0, \quad v_p = p/m \quad (6)$$

The solution of this equation

$$n_F(x, p, t) = n_F(x - v_p t, p, 0) \approx \Theta \left(P_0(x - \frac{p}{m}t) - p \right) \quad (7)$$

shows that a moving Fermi momentum $P_F(x, t)$ obeys a *hodograph* equation

$$P_F(x, t) = P_0(x - P_F(x, t)/m \cdot t) \quad (8)$$

This is Riemann's solution of Euler's equations for hydrodynamics of a compressible one-dimensional fluid, also called Riemann (or Riemann-Burgers, or Riemann-Hopf) equation

$$\partial_t P_F + \nabla E_F = 0, \quad E_F(x, t) = P_F^2(x, t)/2m \quad (9)$$

The Riemann equation leads to shock waves: the velocity of a point with momentum $P_F(x)$ is $P_F(x)/m$: higher parts of the front move faster. The front gets steeper, and eventually attains an infinite gradient – a shock at some finite time. After this moment the Riemann equation has at least three real solutions, $P_{F3}(x, t) > P_{F2}(x, t) > P_{F1}(x, t)$, confined between two turning points $x_-(t), x_+(t)$, the trailing and leading edges respectively (Fig.1).

This phenomena is the gradient catastrophe. Any smooth disturbance of the Fermi surface eventually arrives to a point where the Fermi surface acquires infinite gradients, and then becomes multi-valued between moving turning points x_{\pm} . We focus on that region, namely the region where all electronic states with energy below E_{F1} and between E_{F2} and E_{F3} are occupied. The Fermi distribution acquires at least three, or more edges.

5. Slowly evolving Fermi edges Away from turning points we can employ the Whitham averaging method known in the theory of non-linear waves [19]. The method has been applied to electronic systems in [10]. It is based on a separation of scales between the slowly varying Fermi points and fast oscillations of the electronic states. In short, the Whitham method suggests treating the slowly changing Fermi edges as constants while computing Green's function (2), and then to include the motion of the Fermi edges in the final result. Motion of the Fermi edges is determined by the Riemann equation (9). This approach is valid away from turning points [21]). It can be justified mathematically using an integrable non-linear equation for Green's function obtained in [11]. We omit the mathematical justification of this procedure since the approximation of slowly moving Fermi-edges is physically obvious.

In the shock region $x_- < x_0 < x_+$ we must evaluate the current (2) over a state with three Fermi edges,

where electrons occupy states below E_{F1} and between E_{F2} and E_{F3} , and then treat the time dependent edges as solutions of the hodograph equation (8). This is a non-equilibrium (and stationary FES problem) addressed in Refs. [12–15].

6. Fermi edge resonances Now we are ready to present our result: the current at a frequency close to the edges $\hbar\omega \ll \epsilon_i (\hbar\omega - E_{Fi}) \ll v_F P_0$, in units of cut-offs reads:

$$I(\omega, t) \propto |\hbar\omega - E_{Fi}|^{3a^2 - 2\epsilon_i a} \prod_{j \neq i} E_{ij}^{-2\epsilon_j a} \prod_{n > m} E_{nm}^{2\epsilon_n \epsilon_m a^2}, \quad (10)$$

where $\epsilon_i = (-1)^{i+1}$, $i = 1, 2, 3$ and $E_{ij} = E_{Fi} - E_{Fj}$. The Fermi energies all depend on space-time according to the hodograph equation (8). We suppress this dependence in the notations.

The last factor in this equation gives an overlap between states before and after the shake-up - an Orthogonality Catastrophe formula for multiple edges

$$|\langle \Omega | \Omega' \rangle| = \Delta^{3a^2} \prod_{n > m} E_{nm}^{\epsilon_n \epsilon_m a^2}, \quad (11)$$

where Δ is a level spacing. It is a power of Cauchy determinant $\det \frac{\Delta}{E_{2i+1} - E_{2j}} = \Delta^3 \prod_{n > m} E_{nm}^{\epsilon_n \epsilon_m}$ constructed out of lower and upper edges of occupied bands. These formulas extend the result in [1–3] to multiple edges (see also [12–15]).

If the potential is attractive $a > 0$ (a common case) the current features a peak at E_{F1} (almost zero bias) and an additional resonance at E_{F3} with a power law to the right of the edges. Current is suppressed at the edge E_{F2} . If potential is repulsive $a < 0$ a peak may appear at the edge E_{F2} with a power law to the left to the edge Fig.2.

Apart from additional resonances, the unique features of the shock region is the value of the exponent and the time-dependent amplitudes. Outside of the shock region where there is only one Fermi edge or at a larger energy $|E_{Fi} - E_{Fj}| \ll |\omega - E_F| \ll \Lambda$ where the fine structure of Fermi edges becomes negligible, the current is given by the standard formula [1, 2] $I(\omega) \propto (\omega - E_F)^{a^2 - 2a}$ where only the edge E_F depends on time.

7. Bosonic representation for non-equilibrium states Techniques developed in Refs. [12–15] allow computing the details of the FES resonances. However the most interesting singular power law asymptote next to the edges can be captured by a simpler approach which extends the familiar representation of electronic operators through Bose fields [18]. We briefly discuss it below.

First we separate fast oscillatory modes at each edge

$$c(t, x_0) = \sum_i e^{\frac{i}{\hbar} P_{Fi} x(t)} \psi_i(t)$$

where $\psi_i(t)$ are slowly changing modes and $x(t) = x_0 - v_F t$. Then we represent each slow modes through com-

ponents of the Bose field as

$$\psi_i \propto (\varepsilon_i \prod_{j \neq i} E_{ij}^{\varepsilon_j})^{1/2} e^{-\varepsilon_i \varphi_i}. \quad (12)$$

Under this representation gradients of components of the Bose field

$$\partial_x \varphi_i = i \psi_i^\dagger(t) \psi_i(t), \quad \varphi = \sum_i \varphi_i. \quad (13)$$

are density of slow electronic modes. The Bose field is a sum of its components. The origin of the important factor in front of $e^{-\varepsilon_i \varphi_i}$ will be clear in a moment.

The component of the Bose field represent particle-holes excitations close to each edge. At $\tau E_{ij} \gg \hbar$ they can be treated as independent canonical Bose fields. Their variances $C_i(t_1, t_2) = -\frac{1}{2} \langle \Omega | (\varphi_i(t_2) - \varphi_i(t_1))^2 | \Omega \rangle$ are not difficult to compute. As follows from (13): C_i are electronic density correlations at each edge; C_1 and C_3 are sums of $(\cos \varepsilon \tau - 1)/\varepsilon$ over all possible energies of particle-hole excitations provided that a particle is taken out from the first band $\varepsilon < E_{F1}$ and the second band $E_{F2} < \varepsilon < E_{F3}$ respectively. Similarly C_2 is the sum over momentum of a hole particle excitations provided that a hole is taken out from the "gap" between E_{F1} and E_{F2} . For example $C_2 = \left(\sum_{\varepsilon > 0}^{E_{21}} - \sum_{E_{32}}^{\Lambda} \right) (\cos \varepsilon \tau - 1)/\varepsilon$. Computing these integrals at $\tau \gg \hbar/|E_{ij}|$ one obtains

$$C_i(\tau) = -\log \tau + \varepsilon_i \sum_{j \neq i} \varepsilon_j \log |E_{ij}| \quad (14)$$

The τ -independent term in (14) (a zero mode of the Bose field) explains the pre-factor in (12). Together (12) and (14) produce a canonical electronic correlation function

$$\langle \Omega | \psi_i^\dagger(t_1) \psi_i(t_2) | \Omega \rangle \propto \frac{\varepsilon_i}{x(\tau)} \left(\prod_{j \neq i} E_{ij}^{-\varepsilon_j \varepsilon_i} \right) e^{C_i}. \quad (15)$$

In the Bose representation, Green's function (4) is a sum of edge components

$$G(t_1, t_2) = \sum_i \left(\varepsilon_i \prod_{j \neq i} E_{ij}^{-\varepsilon_i \varepsilon_j} \right) e^{\frac{i}{\hbar} E_{Fi} \tau} G_i(t_1, t_2), \quad (16)$$

$$G_i = \langle e^{(\varepsilon_i - a)(\varphi_i(t_2) - \varphi_i(t_1))} \rangle \prod_{j \neq i} \langle e^{-a(\varphi_j(t_2) - \varphi_j(t_1))} \rangle = e^{(\varepsilon_i - a)^2 C_i} e^{a^2 \sum_{j \neq i} C_j} = e^{(1 - 2\varepsilon_i a) C_i} e^C. \quad (17)$$

We obtain Green's function in the form of two factors: 'closed loops' e^C where each edge contributes equally and 'open lines' L_i corresponding to each edge [1].

$$G = e^C \cdot L, \quad C = a^2 \sum_i C_i, \quad L = \sum_i L_i, \quad (18)$$

$$L_i = \varepsilon_i e^{\frac{i}{\hbar} E_{Fi} \tau} \prod_{j \neq i} E_{ij}^{-\varepsilon_j \varepsilon_i} e^{(1 - 2\varepsilon_i a) C_i}, \quad (19)$$

$$C = -3a^2 \log \tau + a^2 \sum_{j \neq i} \varepsilon_i \varepsilon_j \log |E_{ij}| \quad (20)$$

This prompts the formula for the current (10).

Acknowledgment The authors acknowledge discussions with A. Abanov on all aspects of this work. P. W. was supported by NSF DMR-0906427, MRSEC under DMR-0820054. E. B. was supported by grant 206/07 from the ISF.

-
- [1] P. Nozières, C.T. De Dominicis, Phys.Rev. 178, 1097 (1969)
- [2] G. D. Mahan, Phys. Rev. 163, 612 (1967)
- [3] K. Ohtaka, Y. Tanabe Phys. Rev. B 30, 4235 (1984)
- [4] A. K. Geim, et al., Phys. Rev. Lett. 72, 2061 (1994)
- [5] D. H. Cobden, B. A. Muzykantskii, Phys. Rev. Lett. 75, 4274 (1995)
- [6] I. Hapke-Wurst, et.al., Phys. Rev. B 62 12621 (2000)
- [7] Yu. N. Khanin, et.al., JETP, 105, 152 (2007)
- [8] K.A. Matveev, A.I. Larkin, Phys. Rev. B 46, 15337 (1992)
- [9] P.W. Anderson, Phys. Rev. Lett. 18 1049 (1967)
- [10] E. Bettelheim, A. G. Abanov, P. Wiegmann, Phys. Rev. Lett. 97, 246402 (2006)
- [11] E. Bettelheim, A. G. Abanov, P. Wiegmann J. Phys. A41 (2008) 392003
- [12] M. Combescot and C. Tanguy, Phys. Rev. B, 50, 11484, (1994) C. Tanguy and M. Combescot *ibid* 11499, (1994), *ibid* 52, 11698, (1995)
- [13] D. A. Abanin, L. S. Levitov, Phys. Rev. Lett. 93, 126802 (2004)
- [14] D. B. Gutman, Y. Gefen, A. D. Mirlin. *ArXiv e-prints 1010.5645*, 2010
- [15] E. Bettelheim, Y. Kaplan, P. Wiegmann, *ArXiv e-prints 1103.4236*, 2011
- [16] J. Keeling, I. Klich and L. S. Levitov, Phys. Rev. Lett. 97, 116403 (2006)
- [17] Importance of the spectrum curvature at the Fermi surface has been also emphasized in M. Pustilnik, M. Khodas, A. Kamenev, and L. I. Glazman, Phys. Rev. Lett. 96, 196405 (2006)
- [18] K.D. Schotte, U. Schotte, Phys. Rev. 182,479 (1969)

- [19] G. B. Whitham, Linear and nonlinear waves. John Wiley & Sons Inc., 1999
- [20] For a more detailed study of the Wigner function for semiclassical Fermi states see E. Bettelheim, P. Wiegmann, to be published.
- [21] At turning points where gradients are of the order of a Fermi scale enhanced quantum corrections blur Fermi edges [20].